Article

# Molecular Level Insight into Cellulose Dissolution Mechanism in Carboxylic Acid-Based Deep Eutectic Solvent: A Clue To Understanding Limited Cellulose Solubility In Deep Eutectic Solvents

Mostafa Akhlaghi Bagherjeri , Hassan Monhemi , Abu Naser Md Ahsanul Haque , Maryam Naebe *

Posted Date: 1 November 2024

doi: 10.20944/preprints202411.0045.v1

Keywords: deep eutectic solvents; carboxylic acid; cellulose, hydrogen bonding, molecular dynamics simulation

*Article*

# Molecular Level Insight into Cellulose Dissolution Mechanism in Carboxylic Acid-Based Deep Eutectic Solvent: A Clue To Understanding Limited Cellulose Solubility In Deep Eutectic Solvents

**Mostafa Akhlaghi Bagherjeri [1], Hassan Monhemi [2], Abu Naser Md Ahsanul Haque [1] and Maryam Naebe [1,*]**

[1] Deakin University, Institute for Frontier Materials, Geelong, Victoria 3216, Australia
[2] Department of Chemistry, University of Neyshabur, Neyshabur, Iran
* Correspondence: maryam.naebe@deakin.edu.au

**Abstract:** There is considerable interest in cellulose solubilisation in deep eutectic solvents (DESs) as a new emerging class of green solvents. However, the experimental data have indicated that cellulose is almost insoluble in most of DESs. Carboxylic acid-based DESs are a category of DESs that exhibit a modest ability to solubilise cellulose. However, the molecular-level reasons why carboxylic acid-based DESs can dissolve cellulose are unknown. Such information is crucial in developing DESs with enhanced cellulose solubilising ability. Here, we use molecular dynamics simulations to explore the molecular mechanism of cellulose solubility in oxaline (choline chloride/oxalic acid) as a typical carboxylic acid-based DES and cellulose insolubility in reline (choline chloride/urea) as the most famous DES. It was revealed that oxalic acid possesses a greater ability to weaken the interaction between the chloride anion and the choline cation when compared to urea in reline. Self-interactions of hydrogen bond donors are also highly attenuated in oxaline than in reline. These results explain the observed more significant melting point depression of oxaline in comparison to reline. We depict a molecular mechanism indicating how oxalic acid synergically works with chloride ion to dissolve cellulose and why urea cannot play such a role in reline.

**Keywords:** deep eutectic solvents; carboxylic acid; cellulose; hydrogen bonding; molecular dynamics simulation

## 1. Introduction

Cellulose, being the most abundant biopolymer on Earth, has received considerable interest owing to its biocompatibility, biodegradability, renewability, low cost, and widespread availability [1,2]. The dissolution and subsequent regeneration of cellulose are critical stages in numerous industrial processes, including textile and material manufacturing [3–5]. The majority of commonly used effective cellulose solvents are toxic chemicals, demand substantial energy for processing, and/or generate environmentally harmful byproducts [4,6–9]. The utilisation of renewable and biodegradable resources like cellulose in a green solvent creates a completely environmentally friendly and sustainable process [10].

Ionic liquids (ILs) are one of the most extensively studied green solvents for the dissolution of cellulose [11–15]. A variety of ionic liquids containing 1-butyl-3-methylimidazolium cations ($[C_4mim]^+$) were evaluated, encompassing a spectrum of anions ranging from small, hydrogen-bond acceptors ($Cl^-$) to large, noncoordinating anions ($[PF_6]^-$), as well as $Br^-$, $SCN^-$, and $[BF_4]^-$. The highest solubility was achieved using $[C_4mim]Cl$ as the solvent. Viscous solution containing cellulose up to 25 wt % can be formed in chloride-containing ILs, although compositions ranging between 5 and 10 wt % cellulose are more readily prepared [11].The widespread adoption and practical application of ILs face challenges due to their high cost, complex synthesis procedure, limited biodegradability, and low sustainability, thereby raising questions about their environmental friendliness and practicality [16–20].

Deep eutectic solvents (DESs) are emerging as environmentally friendly and affordable replacements for ILs [21,22]. The discovery of deep eutectic mixture formation was initially documented by Abbott et al. in 2003. This phenomenon was observed for specific hydrogen bond donors (HBDs) and acceptors (HBAs) at the eutectic composition, and it played a pivotal role in sparking interest in the exploration of DESs [23]. The emergence of DESs represents a significant breakthrough in 21st-century green and sustainable chemistry [24,25]. DESs have evolved into versatile solvents with a broad spectrum of applications across various fields such as biocatalysts [26,27], materials [28], extractions [29], gas separation and capture [30–32], biomass and polysaccharides processing [33,34].

The use of DESs in the processing of polysaccharides has gained significant attention in recent years [33] with focus on specific polysaccharides, such as chitin [35], starch, and chitosan [36–39]. One of the most captivating research domains in sustainable polysaccharide processing involves the development of DESs with a notable capability to dissolve cellulose [40]. While ILs have demonstrated the ability to dissolve substantial quantities of cellulose, their application at an industrial scale has proven challenging, primarily due to their high cost and limited biodegradability. Like various other domains, DESs have emerged as highly promising alternatives to replace ILs for cellulose dissolution. However, it is worth noting that many efforts to solubilise cellulose in DESs have been met with limited success. [40].

The highest degree of cellulose solubilisation achieved in DESs has been documented in carboxylic acid based DESs. In particular, Malaeke et al. [41] and Zhang et al. [42] have reported 2.57 wt% and 2.54 wt% cellulose solubility in choline chloride/maleic acid and choline chloride/oxalic acid DESs, respectively. Nevertheless, it is important to note that these solubility levels remain considerably lower than those observed ranges (>10 wt%) in typical ILs [41–45]. The underlying molecular factors responsible for the contrast in solubility between carboxylic acid based DESs and other DES classes remain unknown. Gaining insights into the molecular mechanism governing cellulose solubility in carboxylic acid-based DESs, as well as its insolubility in other DES classes like urea-based DESs, can serve a dual purpose. Not only it can provide a better understanding of the reasons behind the limited solubility in DESs, but it can also pave the way for the design of new generations of DESs with improved cellulose solubility.

The fundamental property shared by all classes of DESs is hydrogen bonding. Hydrogen bonding plays a pivotal role in the formation of DES and their microstructure. The charge delocalisation resulting from hydrogen bonding between the hydrogen bond donor (HBD) and hydrogen bond acceptor (HBA) is the primary reason for the reduction in the melting point of the DES mixture compared to the melting points of its components [46]. Additionally, in DES applications, it is not just the presence of hydrogen bonds between the DES components but also the hydrogen bond interactions between the DES and any other materials in the system that can significantly influence the outcome of the process. We have recently showed that the dissolution process of cellulose is influenced by both the interactions between the solvents themselves (solvent-solvent interactions) and the interactions between the solvent and cellulose (solvent-cellulose interactions)[47]. These two sets of interactions collectively play a crucial role in determining the outcome of the dissolution process. Despite the examination of hydrogen bond structure and dynamics in various classes of DESs, these properties remain poorly understood, particularly in the case of carboxylic acid based DESs.

In recent years, molecular dynamics (MD) simulations have proven to be a versatile computational tool for investigating the microstructure, dynamics, and hydrogen bonding in both ILs and DESs [48–53]. MD simulations are also commonly employed to gain insights into the structure and dynamics of biomacromolecules [54,55] in non-aqueous media [56–60]. Specifically, MD simulations have been employed to elucidate the cellulose dissolution mechanism in ILs [61–79]. We have recently introduced the first straightforward molecular mechanism for cellulose dissolution in NMMO monohydrate through the application of MD simulations [47]. In current work, we have

doi:10.20944/preprints202411.0045.v1

conducted extensive MD simulations to compare the hydrogen bonding structure and dynamics within choline chloride/oxalic acid (oxaline) and choline chloride/urea (reline) DESs. These simulations also examine the interactions between these DESs and cellulose, aiming to reveal the molecular basis of cellulose solubility or insolubility in these DESs.

## 2. Methodology

All MD simulations were carried out using the GROMACS (v. 2019.1) software package and repeated multiple times. The well-defined and validated OPLS-AA parameters of Doherty et al. [80] were used as force field parameters of DES components of reline and oxaline (Figure 1(A)). The short-range electrostatic cutoff was set to 1.6 nm while the Particle-Mesh Ewald (PME) [81] summation method was used for the treatment of long-range electrostatics. LINCS method [82] was used to constrain the chemical bonds involving hydrogen atoms. In the initial stage of the simulation, periodic cubic boxes were created, each containing 250 pairs of choline chloride molecules and the corresponding ratio of hydrogen bond donors (HBDs) for each DES (Table 1). During the construction of the simulation boxes, molecules were inserted using a random distribution algorithm. This ensures that the initial positions of the molecules are randomised within the simulation box, avoiding any pre-arranged order that could bias the results. The random placement allows for a more representative simulation of the molecular interactions as they would occur in a natural, disordered state. There are certain limitations when it comes to the size of the system during MD simulations. For this reason, we have opted to use a relatively small bundle of cellulose (hexamer cellulose) for our simulations. The size of the system does not affect the molecular interactions or the result in this study as the objective is solely to compare the potential of two deep eutectic solvents (DESs) for cellulose dissolution. 5000 steps of energy minimisation were performed for each box using a steepest-descent algorithm. After energy minimisation, each box was equilibrated for 100 ps in an NVT ensemble (constant temperature, constant volume) at 300 K. Then, a 100 ps MD simulation was carried out in the NPT ensemble; constant temperature (300 K) and, constant pressure (1 bar). Next, each box was equilibrated for 20 ns in the NPT ensemble at 300 K and 1 bar. Berendsen [83] and velocity rescaling [84] methods were used to fix the pressure and temperature during simulations. All simulations were performed with a 2 fs timestep and were repeated three times to test the convergence of the results. The final simulation boxes are shown in Figure 1 (B). To validate the force field parameters, the density of each box was calculated and compared with experimental values (Table 2). The results show that there are good agreements between experimental and simulation data indicating the validation of force field parameters.

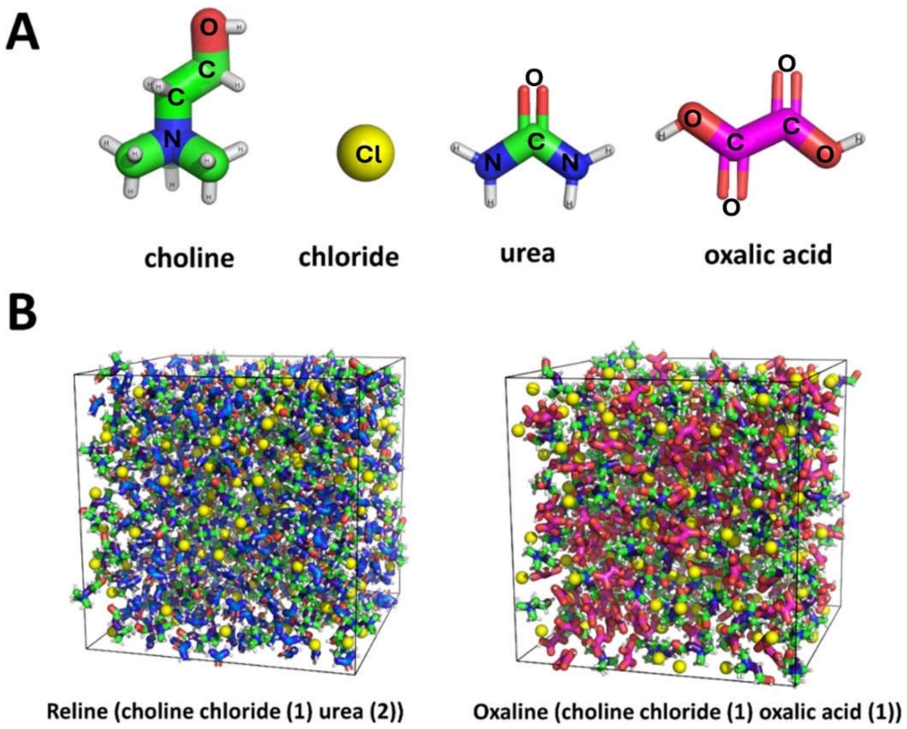

Reline (choline chloride (1) urea (2))

Oxaline (choline chloride (1) oxalic acid (1))

**Figure 1.** (A) structure of DES components in this study and (B) final simulation boxes of reline and oxaline (red: oxygen, blue: nitrogen, green and purple: carbon, chloride: yellow, and hydrogen: grey).

**Table 1.** The number of molecules of each system.

| System | Hexamer cellulose | Choline | $Cl^-$ | Urea | Oxalic acid |
|---|---|---|---|---|---|
| Reline | - | 250 | 250 | 500 | - |
| Oxaline | - | 250 | 250 | - | 250 |
| Cellulose in reline | 4 | 500 | 500 | 1000 | - |
| Cellulose in oxaline | 4 | 500 | 500 | - | 500 |

**Table 2.** The calculated (from simulations) and experimental densities (g/cm$^3$) of reline [85] and oxaline [86]at 298 K.

| DES | Simulation | Experimental |
|---|---|---|
| Reline | 1.182 | 1.198 |
| Oxaline | 1.243 | 1.259 |

To obtain more insights about the interactions in two DESs, the hydrogen bond stabilities were estimated using hydrogen bond time correlation function ($C_{HB}(t)$). $C_{HB}(t)$ is a common hydrogen bond analysis in MD simulations. It is a measure of the hydrogen bond population and decay over time. $C_{HB}(t)$ is defined as:

$$C_{HB}(t)= \frac{<h(0)h(t)>}{<h(0)>} \qquad (1)$$

where h(t) is unity when a particular pair of atoms are hydrogen bonded at time t according to the hydrogen bonding criteria (the distance between the donor and the acceptor should be less than 0.35 nm, and the angle is less than 30 degrees), otherwise h(t) = 0 [87]. A hydrogen bond is defined based on two parameters: the distance between the donor and acceptor atoms, and the angle formed between the donor-hydrogen-acceptor atoms. The angle criterion refers to the angle between the hydrogen atom and the line connecting the donor atom (e.g., oxygen or nitrogen) to the acceptor atom (e.g., oxygen). Typically, the hydrogen bond angle is considered significant if it is within 30° of linearity (i.e., an angle of 150° to 180°)

## 3. Results and Discussion

### 3.1. Hydrogen Bonding Network in Pure Solvents

To gain a deeper understanding of the molecular mechanisms underlying the disparities in cellulose dissolution capabilities between oxaline and reline DESs, we conduct a comprehensive analysis of the hydrogen bond networks established in the pure solvent states as well as in solutions containing cellulose. Since each DES structure contains numerous HBAs and HBDs, it results in intricate hydrogen bond networks unique to each DES. In this context, Sankey diagrams have been employed to illustrate and characterise the quantity and arrangement of diverse hydrogen bonds within reline and oxaline DESs. A Sankey diagram for hydrogen bonds serves as a valuable tool for analysing the topology of hydrogen bond networks in systems featuring multiple and intricate hydrogen bonds [88]. In Figure 2, linear Sankey diagrams are shown illustrating the hydrogen bond networks of pure reline and oxaline. In these diagrams, the hydrogen bond donors are positioned on the left-hand side, while the hydrogen bond acceptors are located on the right-hand side. The numbers within the diagram represent the average hydrogen bond count of the donor or acceptor, and the width of the connection bars is proportional to the number of hydrogen bonds. As depicted in this figure, the hydrogen bond network of both DESs is characterised by a multitude of complex and interconnected hydrogen bonds. It should be noted that in an aqueous environment, water molecules can compete with DES molecules for hydrogen bonding interactions with cellulose. This competition may affect the dissolution behaviour of cellulose in DES aqueous mixtures. The presence of water may hinder or enhance cellulose dissolution depending on the relative strengths of hydrogen bonding interactions between water, DES, and cellulose however, in the designed DESs in this study, no water was involved. Interestingly, despite the distinct properties of reline and oxaline, the hydrogen bond topologies appear to be remarkably similar. Nevertheless, it is important to note that there are variations in the quantity of hydrogen bonds among different components within the DESs. The diagram highlights a prominent observation, which is the central role played by chloride ions in the hydrogen bond networks. It serves as a key acceptor for many hydrogen bonds from both choline (Chl) and HBD (hydrogen bond donors). Chloride ions accept a greater number of interactions in oxaline (5.9) compared to reline (5.01). Notably, in oxaline, chloride ion forms more interaction with HBD but fewer interaction with Chl in comparison to reline. In oxalic acid, hydroxyl oxygen forms a higher number of hydrogen bonds with Chl hydrogen in comparison to the amine nitrogen of urea. Conversely, in reline, the carbonyl oxygen of urea engages a greater number of hydrogen bonds with Chl hydrogen compared to the carbonyl oxygen of oxalic acid in oxaline.

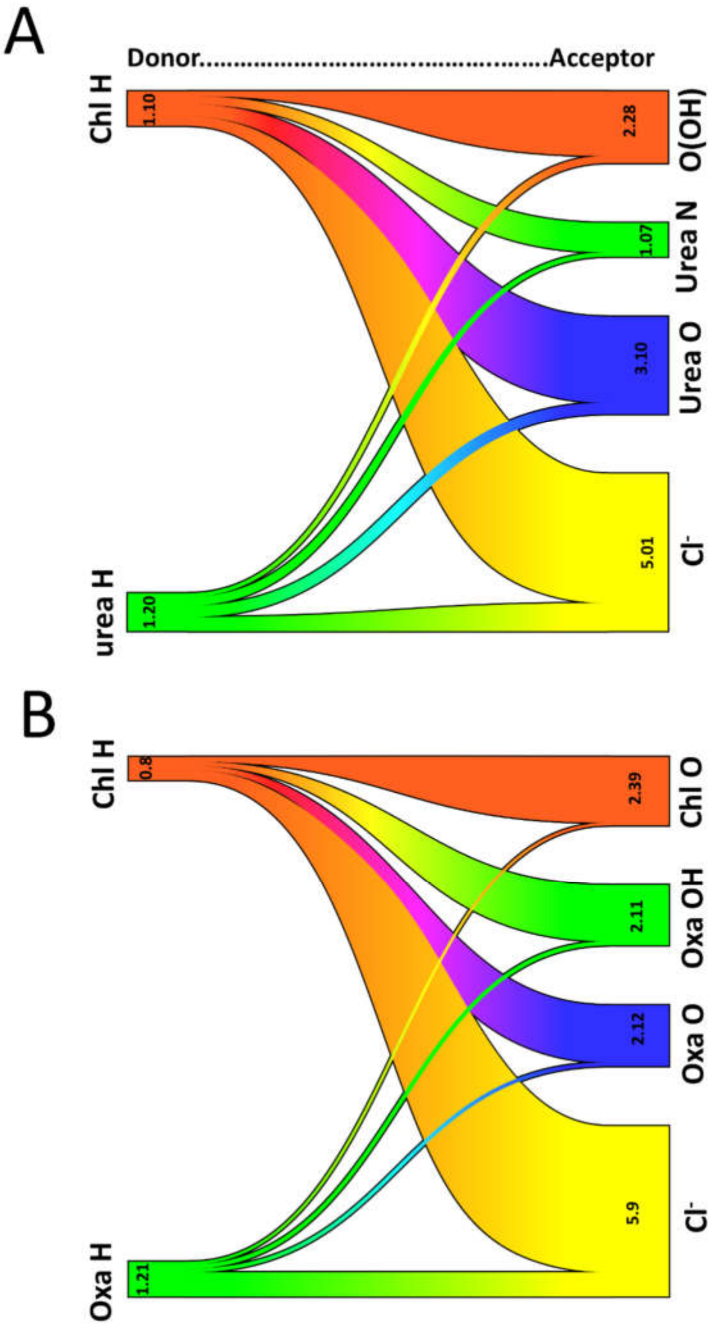

**Figure 2.** Linear Sankey diagram representing the hydrogen bonding topology of (A) reline and (B) oxaline. The numbers represent the average hydrogen bond count for each donor or acceptor.

Although the Sankey diagrams give good information about the total shape of the hydrogen bond network in DESs, to understand the microscopic differences, deeper analysis of each hydrogen bond is needed. The strong interaction formed between Chl and Chloride ions is crucial in choline chloride, contributing significantly to the reinforcement of the crystal structure of this quaternary ammonium salt. As a result, it is anticipated that the interactions of HBD with both choline and chloride ions will have a weakening effect on these two interactions. This weakening is likely to induce alterations in the crystalline structure of ChlCl, lower its melting point, and ultimately lead to the formation of a "deep" eutectic. Hence, the estimation of the structure and strength of the choline-chloride hydrogen bond in each DES can provide insights into the potential of different HBDs to diminish or weaken this interaction. Radial distribution functions (RDFs) can offer more in-depth and intricate insights into the hydrogen bond interactions depicted in Sankey diagrams. In Figure 3,

doi:10.20944/preprints202411.0045.v1

atom-atom RDFs are shown illustrating the relationships between chloride and oxygen atoms of choline, with choline serving as the hydrogen bond donor. These RDFs are presented for both reline and oxaline.

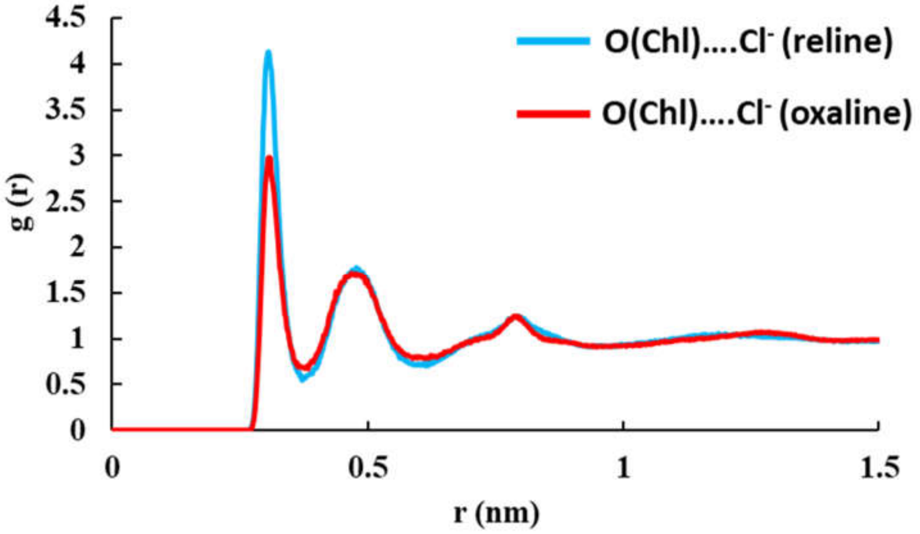

**Figure 3.** Atom-atom RDFs between chloride and oxygen atoms of choline in reline and oxaline.

The radial distribution functions (RDFs) of both solvents exhibit high-intensity first peak at approximately 0.3 nm. Interestingly, the strength of the choline-chloride interaction's first peak is notably reduced in oxaline when compared to reline. This indicates that oxalic acid exerts a more substantial influence on diminishing the strength of the choline-chloride bond when compared with urea. The enhanced capacity of oxalic acid to weaken the choline-chloride interaction can provide a molecular-level explanation for the more pronounced depression in melting point observed experimentally in oxaline, as compared to reline [21,23]. Another important interaction that directly influences the extent of melting point depression in a DES is the self-interaction between hydrogen bond donors (HBD-HBD). Both urea and oxalic acid, which serve as HBDs in reline and oxaline, were in crystalline form before the creation of DESs and therefore have strong hydrogen bond self-interactions. The weakening of HBD-HBD self-interactions, in conjunction with the decrease in choline-chloride interactions, results in the formation of a eutectic mixture. RDFs illustrating the self-interactions of urea and oxalic acid in the corresponding DES are shown in Figure 4.

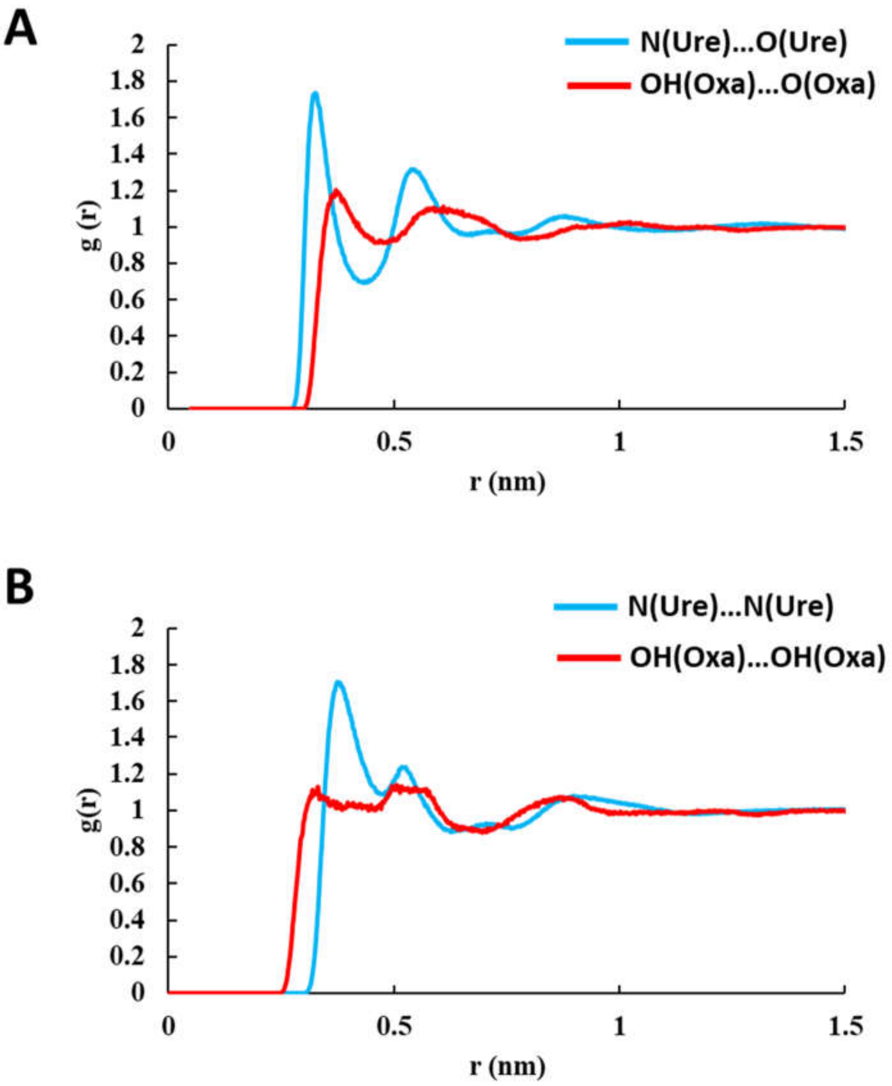

**Figure 4.** Atom-atom RDFs between (A) carbonyl oxygen-hydroxyl hydrogen in oxalic acid/ carbonyl oxygen-amine hydrogen in urea (B) Hydroxyl oxygen-hydroxyl hydrogen in oxalic acid/amine nitrogen-amine hydrogen in urea.

In the HBDs, there are two types of comparable self-interactions involving hydrogen bonds: 1) Carbonyl oxygen-hydroxyl hydrogen in oxalic acid, contrasted with carbonyl oxygen-amine hydrogen in urea, 2) Hydroxyl oxygen-hydroxyl hydrogen in oxalic acid, compared to amine nitrogen-amine hydrogen in urea. As shown in Figure 4, both types of hydrogen bonds exhibit peaks at shorter distances with greater intensities in urea when compared to oxalic acid in their respective DESs. This suggests that the self-interactions between hydrogen bond donors (HBD-HBD) are notably stronger in reline compared to oxaline. In other words, the interactions of chloride and choline ions with HBDs result in a more pronounced reduction of HBD self-interactions in oxaline when compared to reline. This interesting finding, coupled with the results obtained for choline-chloride interactions, provides important insight into the molecular explanations for the more significant melting point depression observed in oxaline compared to reline, starting from their components. To the best of our knowledge, these findings are the first microscopic insights for this important experimental observation in carboxylic acid-based DESs. These results can also be keys to obtaining the molecular basis of observed differences in cellulose dissolution in reline and oxaline which will be discussed in the next sections.

The changes in the internal interactions between choline chloride and HBDs are intricately linked to the interactions of choline and chloride with HBDs within each respective DES. We have calculated RDFs that illustrate potential hydrogen bond interactions for such relationships, guided by the information provided in the Sankey diagrams of the hydrogen bond network. These RDFs are depicted in Figure 5.

The primary and critical hydrogen bond of such interactions is the chloride-HBD hydrogen bond (Figure 5 (A)). Notably, the first peak in the atom-atom RDFs for chloride-HBD interactions occurs at shorter distances with greater intensity in oxaline compared to reline. This suggests a more robust hydrogen bond interaction between chloride and oxalic acid, as compared to chloride and urea in the respective DESs. This hydrogen bond plays a key role in the substantial reduction of internal interactions within choline chloride and HBDs. Stronger interactions of HBD with chloride in oxaline lead to a stronger reduction in both choline-chloride and HBD-HBD interactions and subsequent more melting point depression experimentally seen in oxaline than in reline.

It is important to note that $Cl^-$ can participate in hydrogen bonding, but these bonds are not considered traditional hydrogen bonds as seen with more electronegative atoms like oxygen, nitrogen, or fluorine [89,90]. The $Cl^-$has a lower electronegativity and larger size, which makes its hydrogen bonding interactions weaker and primarily electrostatic in nature rather than purely hydrogen bonding. In the case of $Cl^-$, the hydrogen bonding occurs when the chloride ion interacts with hydrogen atoms that are part of highly polar molecules, typically those where hydrogen is bonded to an electronegative atom like nitrogen or oxygen. While this interaction is sometimes termed a hydrogen bond, it is more accurately described as a charge-assisted hydrogen bond or an electrostatic interaction, due to chloride's negative charge and weaker ability to form strong hydrogen bonds [91,92]. Studies have shown that chloride-hydrogen interactions do occur, especially in the context of ionic liquids and aqueous solutions, but they are often weaker and exhibit different characteristics compared to classic hydrogen bonds [93,94]. These interactions are significant in many solvent systems and biological environments, but they generally lack the directional strength associated with traditional hydrogen bonds.

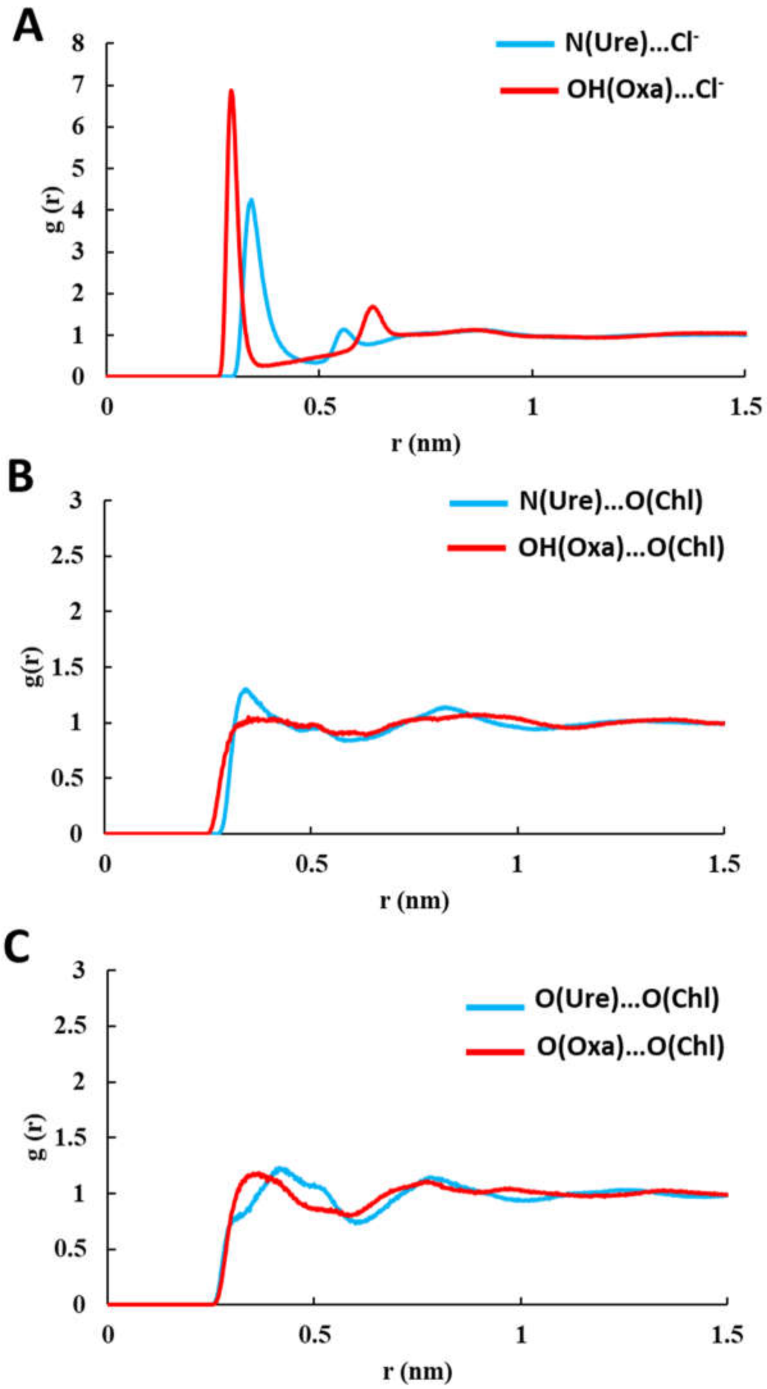

**Figure 5.** Atom-atom RDFs between (A) chloride-amine nitrogen of urea and hydroxyl oxygen of oxalic acid, (B) choline oxygen-amine nitrogen of urea and hydroxyl oxygen of oxalic acid, and (C) choline oxygen-carbonyl oxygen of urea and carbonyl oxygen of oxalic acid.

There are two other important hydrogen bond interactions between ChCl and HBDs (RDFs in Figure 4 (Band C)) including hydrogen bonds of choline hydroxyl with carbonyl and amine of urea and with carbonyl and hydroxyl of oxalic acid. As shown in this figure, both interactions are insignificant and similar in both DESs. Based on these findings, three critical hydrogen bond interactions likely contribute to the distinct behaviors of reline and oxaline: choline-chloride, HBD-chloride, and HBD-HBD interactions. To obtain more insights into these important interactions in two DESs, the hydrogen bond stabilities were estimated from simulation trajectories. As an estimation of hydrogen bond stability, the hydrogen bond time correlation function $C_{HB}(t)$ was calculated for each hydrogen bond. $C_{HB}(t)$ for the most significant distinct hydrogen bonds is depicted in Figure 6. As shown in Figure 6 (A), the stability of the choline-chloride interaction is notably greater in reline compared to oxaline. This finding aligns with the observations in the RDFs shown in Figure 3, emphasising the capacity of oxalic acid to attenuate the interaction between choline and chloride when compared to urea. $C_{HB}(t)$ of hydrogen bonds between HBD and chloride ion is compared in Figure 4 (B). $C_{HB}(t)$ reveals a slower decay for the hydrogen bond between HBD and chloride in oxaline compared to reline. This indicates the stronger nature of this hydrogen bond, which aligns with RDF values observed in Figure 5 (A). The stability of hydrogen bonds relating to self-interactions of HBDs is shown in Figure 6 (C and D). As shown in this figure, hydrogen bonds in both DES are similar and show quick decay. This implies fast hydrogen bond exchanges for HBD-HBD interaction in both DESs.

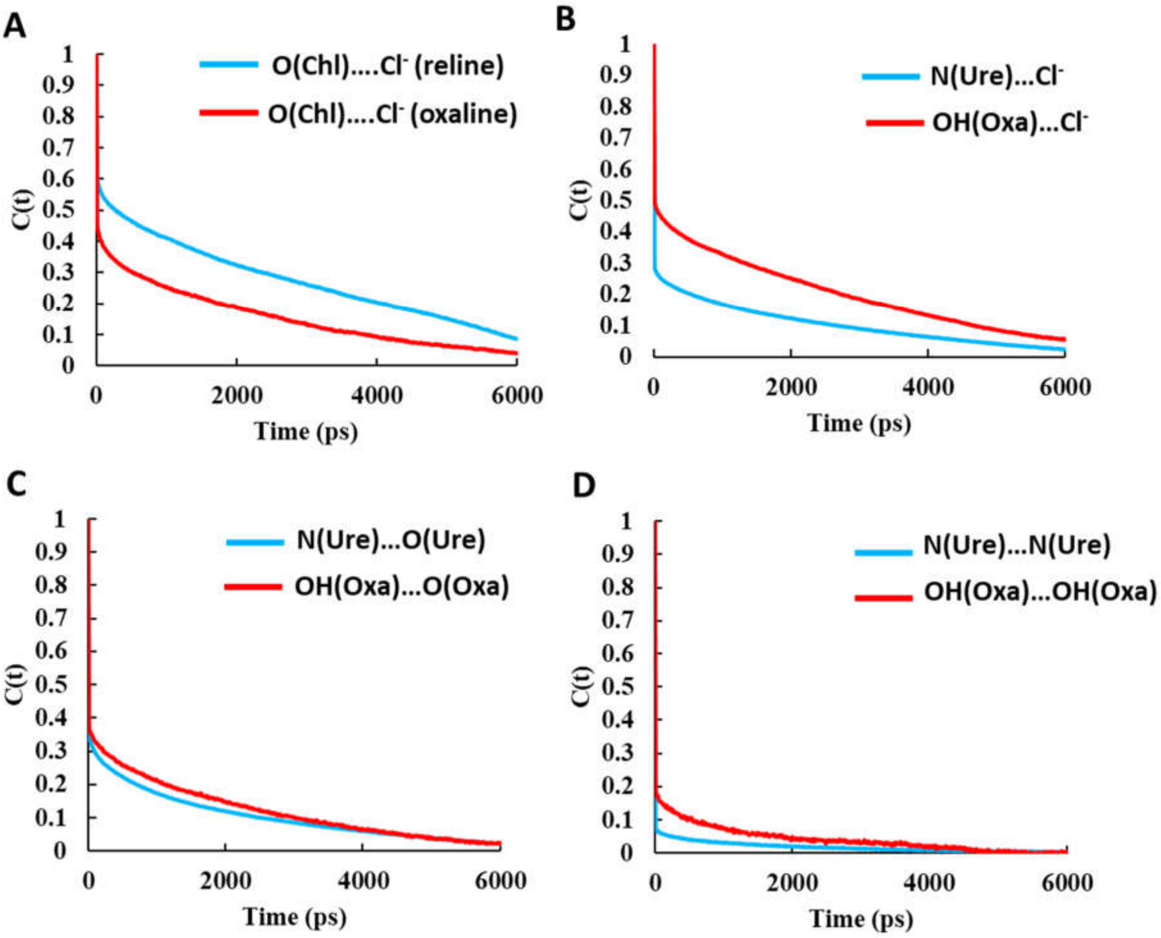

**Figure 6.** Hydrogen bond time correlation function $C_{HB}(t)$ for hydrogen bonds between (A) choline-chloride, (B) HBD-chloride, (C) carbonyl oxygen-hydroxyl hydrogen in oxalic acid/ carbonyl oxygen-amine hydrogen in urea (D) Hydroxyl oxygen-hydroxyl hydrogen in oxalic acid/amine nitrogen-amine hydrogen in urea.

The investigation of hydrogen bonds in pure state of reline and oxaline showed some key facts about the different behaviors of these two solvents: 1) the hydrogen bond interaction between choline and chloride is highly attenuated in oxaline than in reline, 2) there are more significant interactions between HBD and chloride in oxaline than in reline, and 3) HBD-HBD self-interactions are stronger in reline than in oxaline. These three important findings along with simulation data of cellulose in DESs (next section) will be used to depict a molecular basis for cellulose dissolution in DESs.

doi:10.20944/preprints202411.0045.v1

### *3.2. Cellulose-DES Interactions*

To understand the molecular reasons for the greater dissolution capability of oxaline compared to reline, a cellulose bunch including four hexamer cellulose was simulated in reline and oxaline. Here, the cellulose bunch is considered as a crystalline structure, in which the cellulose chains are arranged in a highly ordered manner, representative of a crystalline form of cellulose Iβ. There is no randomness in this arrangement; the crystalline nature ensures that the chains are tightly packed, forming distinct layers through intermolecular hydrogen bonding. The two layers refer to the different planes within this crystalline structure. Figure 7. illustrates the configuration of the initial cellulose bunch structure and provides details regarding the shape and dimensions of the simulation box in reline and Figure 8 represents the graphical representation of the cellulose bunch after 100 ns MD simulation in both reline and oxaline.

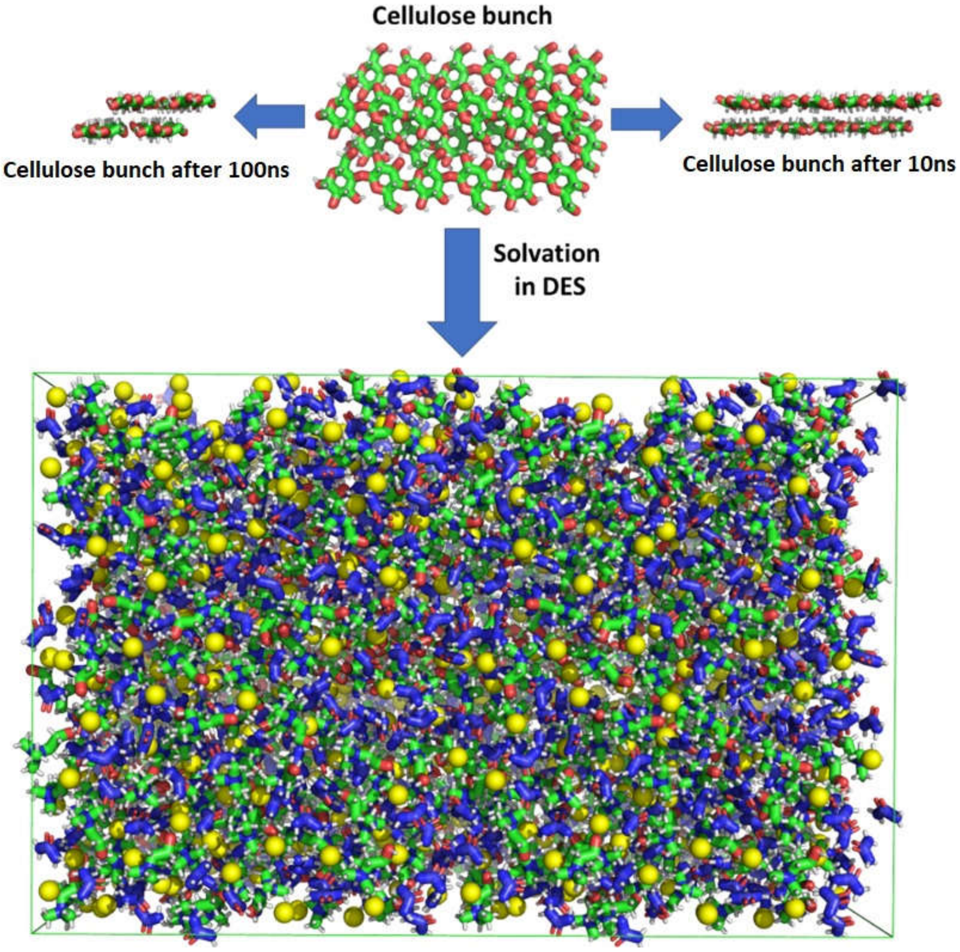

**Figure 7.** Graphical representation of cellulose bunch and its solvation with reline in the simulation box at two different dissolution times.

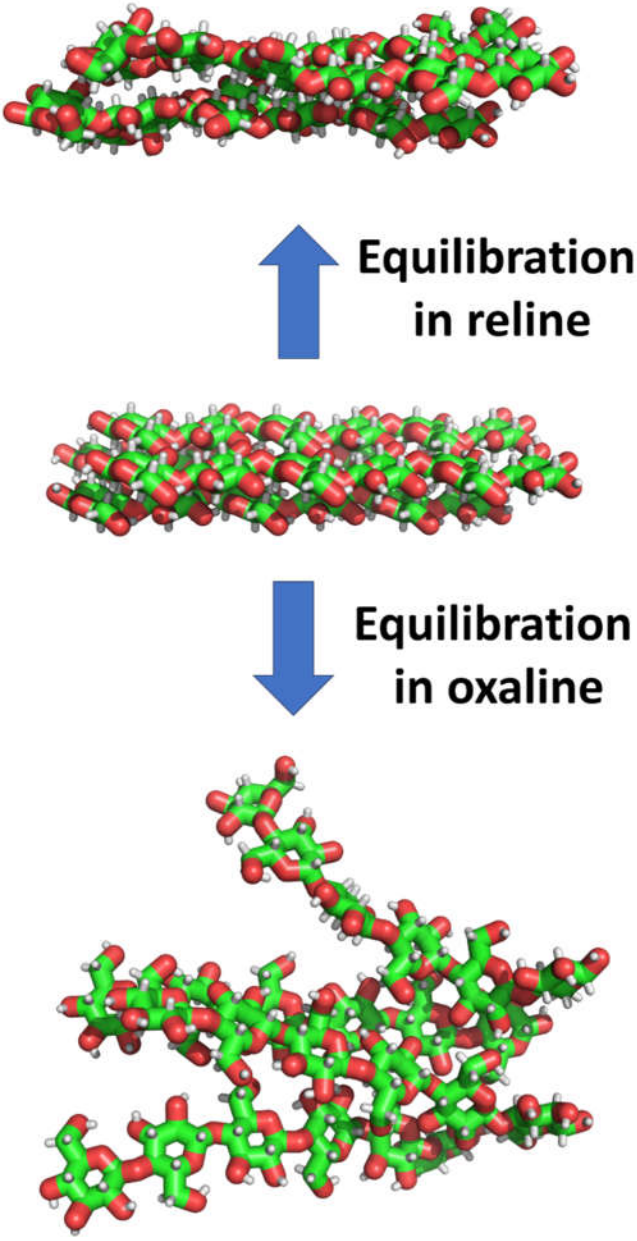

**Figure 8.** Graphical representation of cellulose bunch before and after simulations in reline and oxaline.

As depicted in the figure, the structure of the cellulose bunch remains relatively like its initial configuration in reline. In contrast, the structure of the bunch undergoes decompositions during the 100 ns simulation in oxaline. The root means square deviation (rmsd) values of cellulose structure during the simulations in reline and oxaline are compared in Figure 9 (A)).

doi:10.20944/preprints202411.0045.v1

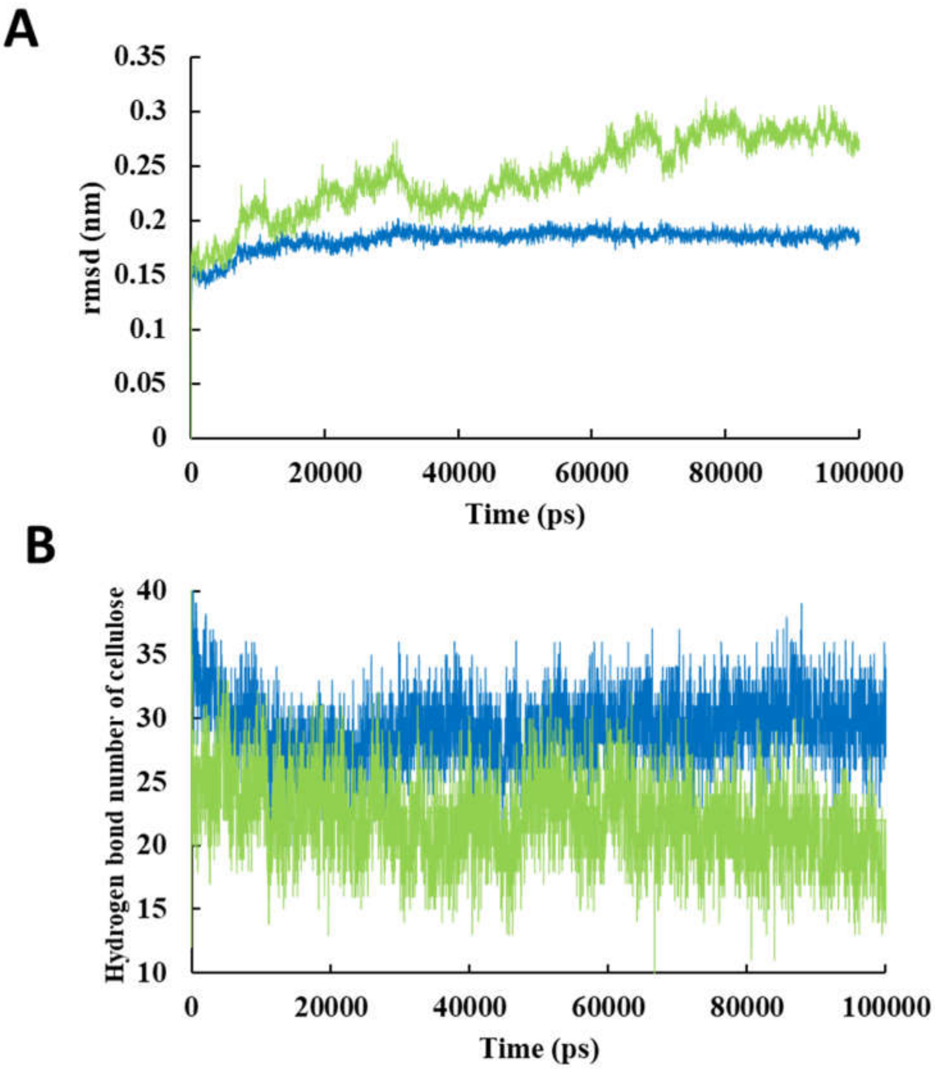

**Figure 9.** (A) The root means square deviation (rmsd) values of cellulose bunch and (B) total hydrogen bonds of cellulose bunch during simulation reline (blue) and oxaline (green). The rmsd applied to all atoms of the cellulose bunch.

In reline, after an initial increase in rmsd (due to a change from crystal state to solution state), the deviations remain constant and stable until the end of simulation time. In contrast, the deviations are severely increased in oxaline in comparison with in reline. The key internal interaction in cellulose structure is hydrogen bonds [95]. The reduction in cellulose hydrogen bonds is an indicator of solubility in different solvents [47,79]. The number of hydrogen bonds in cellulose bunch was calculated during the simulation (Figure 9 (B)). As shown in this figure, the number of hydrogen bonds is relatively constant in reline while gradually decreasing in oxaline. These results agree with the cellulose dissolution ability of oxaline in comparison to cellulose insolubility in reline which was previously reported in experiments. To obtain the molecular basis of the different cellulose solubilities, we have examined the most important interactions that lead to instability and hydrogen bond reduction of the bunch in oxaline and have compared them with the same interactions in reline. The primary interaction in the cellulose dissolution process is solute-solvent hydrogen bonding [79,93]. $O_2$, $O_3$, and $O_6$ atoms of cellulose typically serve as hydrogen bond donors to interact with hydrogen bond acceptors within the solvent. Consequently, to examine the principal hydrogen bonding interactions between cellulose-solvent in reline and oxaline, RDFs between the oxygen atoms of cellulose and the primary hydrogen bond acceptors of reline (chloride ion, urea carbonyl and amine) and oxaline (chloride ion, oxalic acid carbonyl and hydroxyl) have been computed and are compared in Figure 10.

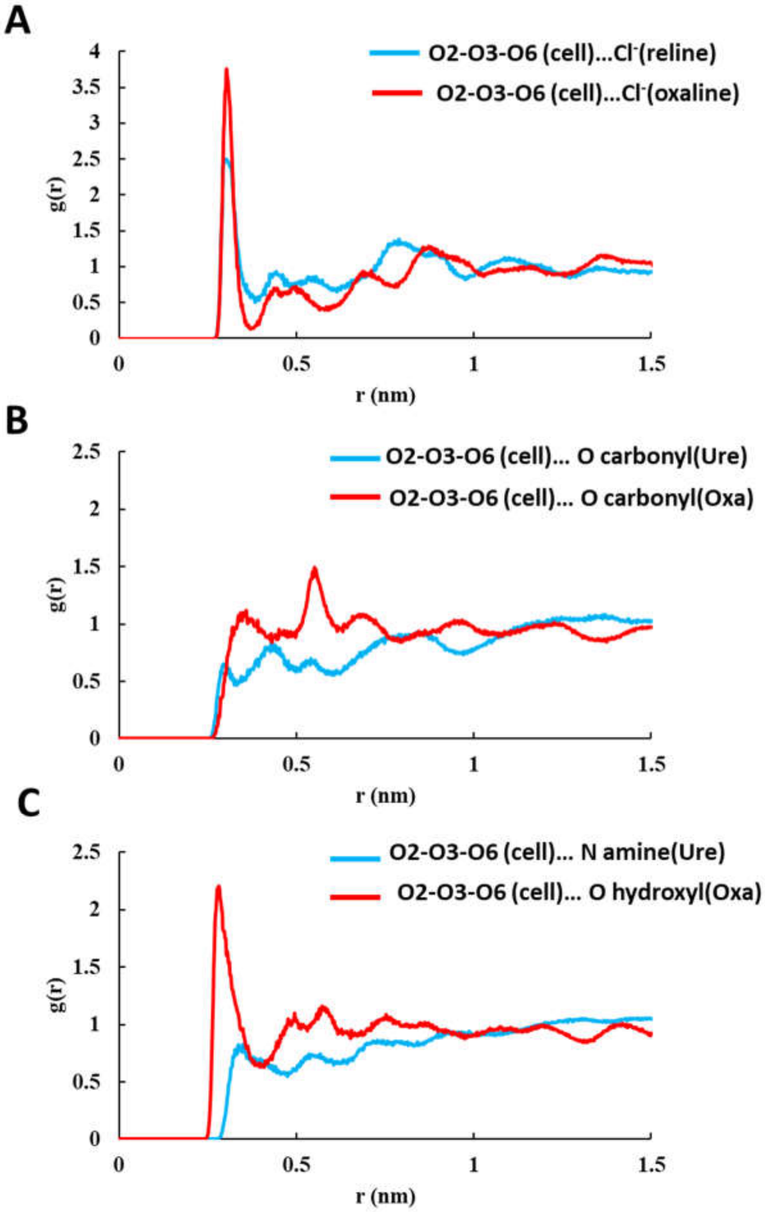

**Figure 10.** Atom-atom RDFs between (A) cellulose O-chloride of reline and oxaline (B) Cellulose O-carbonyl of urea and carbonyl of oxalic acid and (C) cellulose O-amine nitrogen of urea and hydroxyl oxygen of oxalic acid (here, O2, O3, and O6 correspond to the oxygen atoms attached to the hydroxyl groups at positions C2, C3, and C6 of the cellulose backbone, respectively).

Remarkably, the initial peak in the RDFs for all types of hydrogen bonds exhibits greater intensity in oxaline compared to reline. In all three cases, oxaline makes significant interactions with cellulose. In contrast, there are no significant hydrogen bond interactions between reline components and cellulose. These microscopic insights reveal how cellulose can be solubilised in oxaline and not in reline. Interestingly, the interaction of cellulose with oxalic acid hydroxyl groups is unexpectedly stronger than with oxalic acid carbonyl (Figure 10 (B and C)). Therefore, it can be said that the most important interaction sites of cellulose with oxaline are chloride ions and oxalic acid hydroxyl. Apart from chloride ions, the methyl ($CH_3$) groups present on choline have the capability to interact with the hydrophobic ring surfaces of cellulose in oxaline, primarily due to the reduced presence of chloride ions compared to reline which leads to dispersion interaction. Dispersion forces between the methyl groups in oxaline or reline and the hydrophobic regions of cellulose molecules facilitate solvent-solute interactions. These interactions help weaken the intra- and intermolecular hydrogen bonds within cellulose, aiding its dissolution. Also, dispersion forces help to stabilise the dissolved cellulose chains in the solvent, preventing re-aggregation and facilitating dissolution and apparently this positive effect is felt more in oxaline than reline. This could be evident from the difference in the molecular orientation of cellulose bunch before and after simulations in reline and oxaline (Figure 8).To compare the stability of hydrogen bonds related to these interactions during cellulose simulations in reline and oxaline, the $C_{HB}(t)$ for the related hydrogen bonds are shown in Figure 11. As shown in this figure, the stability of the hydrogen bonds between the components of DESs and cellulose is notably greater in oxaline than in reline. These findings highlight the crucial roles played by both chloride and oxalic acid in the molecular mechanism of cellulose dissolution in oxaline. Based on the results obtained, we can construct a molecular mechanism for cellulose dissolution in oxaline and elucidate why cellulose can be dissolved in oxaline but not in reline.

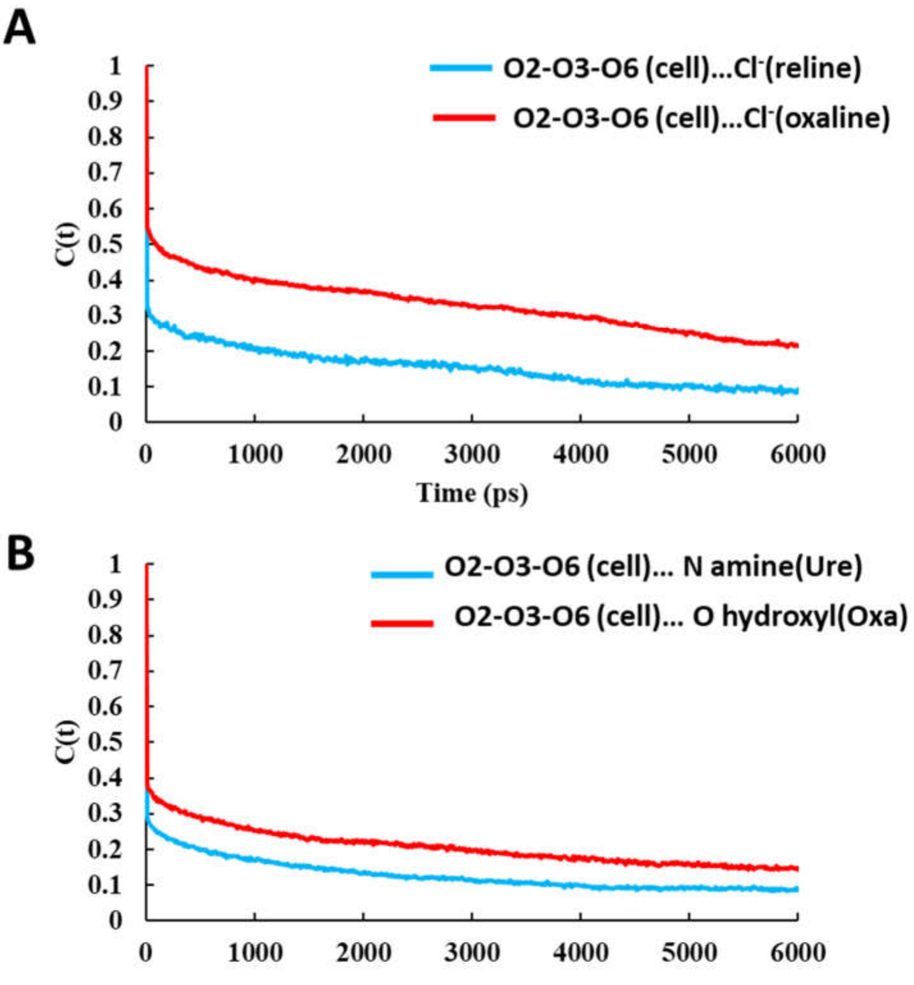

**Figure 11.** Hydrogen bond time correlation function $C_{HB}(t)$ for hydrogen bonds between (A) cellulose O-chloride in reline and oxaline and (B) cellulose O-amine nitrogen of urea and hydroxyl oxygen of oxalic acid.

## 4. Molecular Mechanism of Cellulose Dissolution in Oxaline

In the preceding sections, it was demonstrated that the robust chloride-HBD interaction in oxaline results in reductions in both choline-chloride and HBD-HBD interactions. This notably separates chloride from choline and HBD from other HBDs in oxaline when compared to their initial crystal structures. Hence, it is reasonable to anticipate the formation of a stable complex between oxalic acid and chloride. We believe that the formation of these complexes could play a crucial role in the molecular mechanism of cellulose dissolution in oxalic acid. Due to the strong HBD-HBD and choline-chloride interactions in reline, the formation of these complexes occurs with a lower probability in comparison to what can be seen in oxaline. Considering these findings, we have outlined a stepwise molecular mechanism for cellulose dissolution in oxaline (Figure 12) which is not possible in reline. Due to the smaller size of chloride ions in comparison to choline and HBDs, they can initially diffuse between the cellulose chains and make initial H bonds with cellulose (Figure 12 (A)). This leads to a slight loosening of the strong interactions between cellulose chains. Due to the potent interaction between oxalic acid and chloride ions, oxalic acid can subsequently diffuse to the chloride ion's location and make hydrogen bonds with it in the proximity of cellulose chains (Figure 12 (B)). At the same time, oxalic acid can form hydrogen bonds with the hydroxyl groups in cellulose. This leads to more loosening of cellulose chains. Oxalic acid can make hydrogen bonds (through its hydroxyls) with both chloride and cellulose which is a key step in cellulose unzipping (Figure 12 (C)). Additional chloride ions can diffuse towards the cellulose chains to engage in interactions with both the hydroxyl groups of oxalic acid and those of cellulose. This leads to the gradual formation of the complex described earlier, consecutively between cellulose chains. Choline molecules may also diffuse among cellulose chains engaging in interactions with chloride, oxalic acid, and cellulose. However, owing to its considerable size, the diffusion of choline molecules among cellulose chains may take place during the later stages of cellulose unzipping. Moreover, some other works reported delayed diffusion by larger molecules in ionic liquids and their interactions with cellulose. For example, Y. Li et al [93] reported that choline ions, due to their relatively larger size, typically exhibit slower diffusion compared to smaller species like chloride or urea. This behaviour is observed in many ionic liquids and DESs, where the smaller ions initiate interaction with cellulose while larger ions follow later in the solvation process. They discussed how cation-anion interactions influence the dissolution process in ionic liquids, with cations like choline playing a key role at later stages due to their size. Similar observations are reported in the work by X. Yuan and G. Cheng [96] which explored the solvation and dissolution mechanisms of cellulose in ionic liquids. The study highlights how larger cations like imidazolium diffuse into cellulose networks after smaller ions initiate disruption of the cellulose hydrogen bonding network. These studies align with the explanation provided regarding the delayed diffusion of larger molecules like choline during the cellulose unzipping process. Given the robust self-interactions observed in choline-chloride and urea-urea interactions, the formation of a chloride-urea complex and the subsequent unzipping of cellulose probably occurred to a lesser extent which is not enough for cellulose solubilising. We have recently explored a similar molecular mechanism for NMMO monohydrate [47]. We found that in NMMO monohydrate, self-interaction of NMMO-NMMO was the key to the molecular mechanism of cellulose dissolution. Here, oxalic acid-chloride interaction plays a pivotal role in the dissolution mechanism. This molecular representation not only explains the molecular basis of different cellulose solubility in oxaline and reline, but it also outlines the inaugural molecular mechanism for cellulose dissolution in DESs. Furthermore, this insight can facilitate the development of novel DES systems with enhanced cellulose solubility. The design of choline chloride-based DESs with improved cellulose dissolution capabilities is closely linked to the characteristics of their HBDs. An effective HBD for choline chloride based DESs should possess several key attributes. Firstly, it should be able to strongly attenuate choline-chloride interactions. Secondly, it forms robust interactions with chloride ions. Finally, it contains multiple hydrogen bond acceptors within its structure. These properties are very helpful in designing DESs with heightened cellulose dissolution abilities.

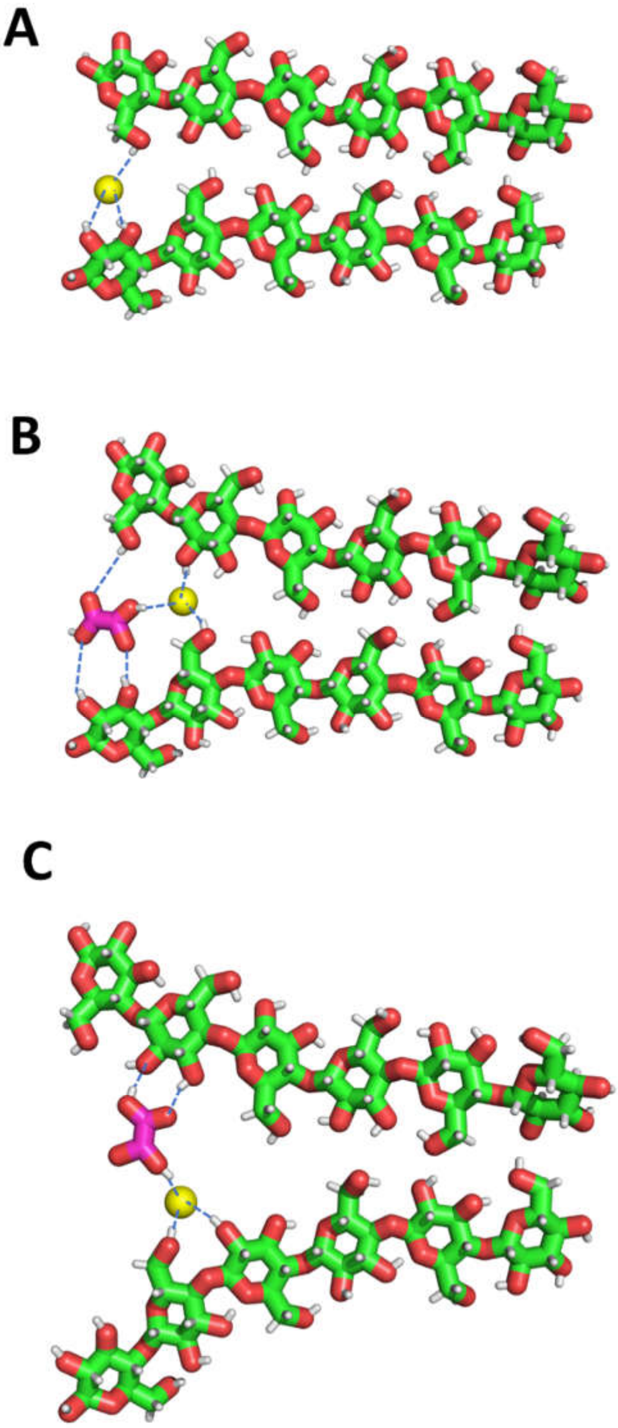

**Figure 12.** Molecular mechanism of cellulose dissolution in oxaline (A) chloride ion establishes H bonds with cellulose chain which leads to initial loosening of cellulose chain (B) due to strong interaction between chloride and hydroxyl of oxalic acid, oxalic acid diffuses between chains which leads to further loosening, (C) oxalic acid interacts with both chloride and cellulose through its hydroxyls which is important step in cellulose unzipping (dashed lines show H bonds).

## 5. Conclusions

Despite substantial efforts and interest in developing customised DESs for cellulose dissolution, this research field has encountered limited success so far. Carboxylic acid-based DESs, especially those derived from choline chloride and oxalic acid, are some of the relatively few DESs that exhibit restricted cellulose solubility. However, the molecular basis of cellulose solubility in this DES class is almost unknown. By conducting a comparative analysis of the microstructure, hydrogen bonds, and their interactions with cellulose in DESs characterised by limited cellulose solubility, like choline chloride/urea (reline) and choline chloride/oxalic acid (oxaline), our objective was to unveil the molecular foundation for this limited solubility in deep eutectic solvents. Furthermore, we intended to outline a molecular mechanism for cellulose solubility within oxalic acid-based DESs. Molecular dynamics simulations of this system demonstrated that within DESs, HBDs may play a critical role. They achieved this by forming strong interactions with chloride ions and choline, effectively weakening choline-chloride interactions. These also led to weakening HBD-HBD interactions. These phenomena resulted in both chloride ions and HBDs being liberated from internal interactions with other components of the DES. This newfound freedom allows them to establish multiple hydrogen bonds with cellulose. We have effectively illustrated how this molecular representation is feasible in oxaline but not in reline, potentially assisted by the dispersion interaction governed by the $CH_3$ groups of choline which were more free in oxaline than reline. Ultimately, we have outlined a clear and direct molecular mechanism for cellulose dissolution in oxaline. We have elucidated how oxalic acid and chloride ions synergically function to dissolve cellulose in oxaline. The important properties that make a HBD suitable for cellulose dissolution were summarised as: the ability to attenuate choline-chloride interactions, forming strong interactions with chloride ions, and having multiple hydrogen bond acceptors within its structure. We believe that these significant microscopic revelations not only resolve certain ambiguities in cellulose/DES systems but also have the potential to open new and promising avenues for designing novel DESs with enhanced cellulose dissolution capabilities. As a next step of this work, the impact of different temperatures and the generation of free energy in the system towards the cellulose solubility will be analysed to further validate the results.

**Author Contributions: M.A.B.:** Conceptualisation, Investigation, Writing—original draft, Writing—review & editing; **H.M.:** Conceptualisation, Methodology, Writing—review & editing**; A.N.M.A.H.:** Writing—review & editing**; M.N.:** Writing—review & editing, funding acquisitions**.** All authors have read and agreed to the published version of the manuscript.

**Conflicts of Interest:** The authors declare no conflict of interest.

**Funding:** No funding reported.

**Data Availability Statement:** Data will be available upon request.

**Acknowledgments:** The current study was supported by the Deakin University Postgraduate Research Scholarship (DUPRS). The authors acknowledge the support from the Australian Research Council ITRH (IH210100023).

## References

1. [1] D. Klemm, B. Heublein, H.-P. Fink, A. Bohn, Cellulose: Fascinating Biopolymer and Sustainable Raw Material, Angewandte Chemie International Edition 44(22) (2005) 3358-3393.
2. [2] J.T. McNamara, J.L. Morgan, J. Zimmer, A molecular description of cellulose biosynthesis, Annu Rev Biochem 84 (2015) 895-921.
3. [3] S. Acharya, S. Liyanage, P. Parajuli, S.S. Rumi, J.L. Shamshina, N. Abidi, Utilization of Cellulose to Its Full Potential: A Review on Cellulose Dissolution, Regeneration, and Applications, Polymers (Basel) 13(24) (2021).
4. [4] A.J. Sayyed, N.A. Deshmukh, D.V. Pinjari, A critical review of manufacturing processes used in regenerated cellulosic fibres: viscose, cellulose acetate, cuprammonium, LiCl/DMAc, ionic liquids, and NMMO based lyocell, Cellulose 26(5) (2019) 2913-2940.
5. [5] B. Medronho, B. Lindman, Brief overview on cellulose dissolution/regeneration interactions and mechanisms, Advances in Colloid and Interface Science 222 (2015) 502-508.
6. [6] A. Isogai, R.H. Atalla, Dissolution of Cellulose in Aqueous NaOH Solutions, Cellulose 5(4) (1998) 309-319.
7. [7] J. Cai, L. Zhang, Rapid Dissolution of Cellulose in LiOH/Urea and NaOH/Urea Aqueous Solutions, Macromolecular Bioscience 5(6) (2005) 539-548.

8. [8] A.-L. Dupont, Cellulose in lithium chloride/N,N-dimethylacetamide, optimisation of a dissolution method using paper substrates and stability of the solutions, Polymer 44(15) (2003) 4117-4126.
9. [9] S. Zhang, F.-X. Li, J.-y. Yu, Y.-L. Hsieh, Dissolution behaviour and solubility of cellulose in NaOH complex solution, Carbohydrate Polymers 81(3) (2010) 668-674.
10. [10] L. Soh, M.J. Eckelman, Green Solvents in Biomass Processing, ACS Sustainable Chemistry & Engineering 4(11) (2016) 5821-5837.
11. [11] R.P. Swatloski, S.K. Spear, J.D. Holbrey, R.D. Rogers, Dissolution of cellose with ionic liquids, Journal of the American chemical society 124(18) (2002) 4974-4975.
12. [12] H. Wang, G. Gurau, R.D. Rogers, Ionic liquid processing of cellulose, Chemical Society Reviews 41(4) (2012) 1519-1537.
13. [13] S. Zhu, Y. Wu, Q. Chen, Z. Yu, C. Wang, S. Jin, Y. Ding, G. Wu, Dissolution of cellulose with ionic liquids and its application: a mini-review, Green Chemistry 8(4) (2006) 325-327.
14. [14] M. Isik, H. Sardon, D. Mecerreyes, Ionic liquids and cellulose: dissolution, chemical modification and preparation of new cellulosic materials, Int J Mol Sci 15(7) (2014) 11922-40.
15. [15] C. Verma, A. Mishra, S. Chauhan, P. Verma, V. Srivastava, M.A. Quraishi, E.E. Ebenso, Dissolution of cellulose in ionic liquids and their mixed cosolvents: A review, Sustainable Chemistry and Pharmacy 13 (2019) 100162.
16. [16] J. Flieger, M. Flieger, Ionic Liquids Toxicity—Benefits and Threats, International Journal of Molecular Sciences, 2020.
17. [17] D. Coleman, N. Gathergood, Biodegradation studies of ionic liquids, Chemical Society reviews 39 (2010) 600-37.
18. [18] J. Zhao, M.R. Wilkins, D. Wang, A review on strategies to reduce ionic liquid pretreatment costs for biofuel production, Bioresource Technology 364 (2022) 128045.
19. [19] L. Chen, M. Sharifzadeh, N. Mac Dowell, T. Welton, N. Shah, J.P. Hallett, Inexpensive ionic liquids: [HSO4]−-based solvent production at bulk scale, Green Chemistry 16(6) (2014) 3098-3106.
20. [20] S.K. Singh, A.W. Savoy, Ionic liquids synthesis and applications: An overview, Journal of Molecular Liquids 297 (2020) 112038.
21. [21] A.P. Abbott, D. Boothby, G. Capper, D.L. Davies, R.K. Rasheed, Deep Eutectic Solvents Formed between Choline Chloride and Carboxylic Acids:  Versatile Alternatives to Ionic Liquids, Journal of the American Chemical Society 126(29) (2004) 9142-9147.
22. [22] B. Nian, X. Li, Can deep eutectic solvents be the best alternatives to ionic liquids and organic solvents: A perspective in enzyme catalytic reactions, International Journal of Biological Macromolecules 217 (2022) 255-269.
23. [23] A.P. Abbott, G. Capper, D.L. Davies, R.K. Rasheed, V. Tambyrajah, Novel solvent properties of choline chloride/urea mixtures, Chemical Communications (1) (2003) 70-71.
24. [24] A. Paiva, R. Craveiro, I. Aroso, M. Martins, R.L. Reis, A.R.C. Duarte, Natural Deep Eutectic Solvents – Solvents for the 21st Century, ACS Sustainable Chemistry & Engineering 2(5) (2014) 1063-1071.
25. [25] C. Florindo, F. Lima, B.D. Ribeiro, I.M. Marrucho, Deep eutectic solvents: overcoming 21st century challenges, Current Opinion in Green and Sustainable Chemistry 18 (2019) 31-36.
26. [26] M. Pätzold, S. Siebenhaller, S. Kara, A. Liese, C. Syldatk, D. Holtmann, Deep Eutectic Solvents as Efficient Solvents in Biocatalysis, Trends in Biotechnology 37(9) (2019) 943-959.
27. [27] P. Xu, G.W. Zheng, M.H. Zong, N. Li, W.Y. Lou, Recent progress on deep eutectic solvents in biocatalysis, Bioresour Bioprocess 4(1) (2017) 34.
28. [28] D.V. Wagle, H. Zhao, G.A. Baker, Deep Eutectic Solvents: Sustainable Media for Nanoscale and Functional Materials, Accounts of Chemical Research 47(8) (2014) 2299-2308.
29. [29] T. Gu, M. Zhang, T. Tan, J. Chen, Z. Li, Q. Zhang, H. Qiu, Deep eutectic solvents as novel extraction media for phenolic compounds from model oil, Chemical Communications 50(79) (2014) 11749-11752.
30. [30] R.B. Leron, M.-H. Li, Solubility of carbon dioxide in a choline chloride–ethylene glycol based deep eutectic solvent, Thermochimica Acta 551 (2013) 14-19.
31. [31] D. Yang, M. Hou, H. Ning, J. Zhang, J. Ma, G. Yang, B. Han, Efficient SO2 absorption by renewable choline chloride–glycerol deep eutectic solvents, Green Chemistry 15(8) (2013) 2261-2265.
32. [32] S. Sarmad, J.-P. Mikkola, X. Ji, Carbon Dioxide Capture with Ionic Liquids and Deep Eutectic Solvents: A New Generation of Sorbents, ChemSusChem 10(2) (2017) 324-352.
33. [33] M. Zdanowicz, K. Wilpiszewska, T. Spychaj, Deep eutectic solvents for polysaccharides processing. A review, Carbohydrate Polymers 200 (2018) 361-380.
34. [34] Y. Chen, T. Mu, Application of deep eutectic solvents in biomass pretreatment and conversion, Green Energy & Environment 4(2) (2019) 95-115.
35. [35] Z. Li, C. Liu, S. Hong, H. Lian, C. Mei, J. Lee, Q. Wu, M.A. Hubbe, M.-C. Li, Recent advances in extraction and processing of chitin using deep eutectic solvents, Chemical Engineering Journal 446 (2022) 136953.
36. [36] D. Skowrońska, K. Wilpiszewska, Deep Eutectic Solvents for Starch Treatment, Polymers, 2022.

37. [37] E. Leroy, P. Decaen, P. Jacquet, G. Coativy, B. Pontoire, A.-L. Reguerre, D. Lourdin, Deep eutectic solvents as functional additives for starch based plastics, Green Chemistry 14(11) (2012) 3063-3066.
38. [38] K. Wilpiszewska, D. Skowrońska, Evaluation of starch plasticization efficiency by deep eutectic solvents based on choline chloride, Journal of Molecular Liquids 384 (2023) 122210.
39. [39] J. Yu, S. Xu, G. Goksen, C. Yi, P. Shao, Chitosan films plasticized with choline-based deep eutectic solvents: UV shielding, antioxidant, and antibacterial properties, Food Hydrocolloids 135 (2023) 108196.
40. [40] Y.-L. Chen, X. Zhang, T.-T. You, F. Xu, Deep eutectic solvents (DESs) for cellulose dissolution: a mini-review, Cellulose 26(1) (2019) 205-213.
41. [41] H. Malaeke, M.R. Housaindokht, H. Monhemi, M. Izadyar, Deep eutectic solvent as an efficient molecular liquid for lignin solubilization and wood delignification, Journal of Molecular Liquids 263 (2018) 193-199.
42. [42] H. Zhang, J. Lang, P. Lan, H. Yang, J. Lu, Z. Wang, Study on the Dissolution Mechanism of Cellulose by ChCl-Based Deep Eutectic Solvents, Materials (Basel) 13(2) (2020).
43. [43] H. Ren, C. Chen, S. Guo, D. Zhao, Q. Wang, Synthesis of a Novel Allyl-Functionalized Deep Eutectic Solvent to Promote Dissolution of Cellulose, BioResources 11 (2016).
44. [44] H.V.D. Nguyen, R. De Vries, S.D. Stoyanov, Natural Deep Eutectics as a "Green" Cellulose Cosolvent, ACS Sustainable Chemistry & Engineering 8(37) (2020) 14166-14178.
45. [45] V.I.B. Castro, F. Mano, R.L. Reis, A. Paiva, A.R.C. Duarte, Synthesis and Physical and Thermodynamic Properties of Lactic Acid and Malic Acid-Based Natural Deep Eutectic Solvents, Journal of Chemical & Engineering Data 63(7) (2018) 2548-2556.
46. [46] A.P. Abbott, G. Capper, D.L. Davies, H.L. Munro, R.K. Rasheed, V. Tambyrajah, Preparation of novel, moisture-stable, Lewis-acidic ionic liquids containing quaternary ammonium salts with functional side chains, Chemical Communications (19) (2001) 2010-2011.
47. [47] M. Akhlaghi Bagherjeri, H. Monhemi, A.N.M.A. Haque, M. Naebe, Molecular mechanism of cellulose dissolution in N-methyl morpholine-N-oxide: A molecular dynamics simulation study, Carbohydrate Polymers 323 (2024) 121433.
48. [48] S.H. Vahidi, H. Monhemi, M. Hojjatipour, M. Hojjatipour, M. Eftekhari, M. Vafaeei, Supercritical CO2/Deep Eutectic Solvent Biphasic System as a New Green and Sustainable Solvent System for Different Applications: Insights from Molecular Dynamics Simulations, The Journal of Physical Chemistry B 127(37) (2023) 8057-8065.
49. [49] D. Bedrov, J.-P. Piquemal, O. Borodin, A.D. MacKerell, Jr., B. Roux, C. Schröder, Molecular Dynamics Simulations of Ionic Liquids and Electrolytes Using Polarizable Force Fields, Chemical Reviews 119(13) (2019) 7940-7995.
50. [50] S. Tsuzuki, W. Shinoda, H. Saito, M. Mikami, H. Tokuda, M. Watanabe, Molecular Dynamics Simulations of Ionic Liquids: Cation and Anion Dependence of Self-Diffusion Coefficients of Ions, The Journal of Physical Chemistry B 113(31) (2009) 10641-10649.
51. [51] T. Köddermann, D. Paschek, R. Ludwig, Molecular Dynamic Simulations of Ionic Liquids: A Reliable Description of Structure, Thermodynamics and Dynamics, ChemPhysChem 8(17) (2007) 2464-2470.
52. [52] D. Tolmachev, N. Lukasheva, R. Ramazanov, V. Nazarychev, N. Borzdun, I. Volgin, M. Andreeva, A. Glova, S. Melnikova, A. Dobrovskiy, S.A. Silber, S. Larin, R.M. de Souza, M.C. Ribeiro, S. Lyulin, M. Karttunen, Computer Simulations of Deep Eutectic Solvents: Challenges, Solutions, and Perspectives, International Journal of Molecular Sciences, 2022.
53. [53] M. Atilhan, S. Aparicio, Molecular dynamics simulations of mixed deep eutectic solvents and their interaction with nanomaterials, Journal of Molecular Liquids 283 (2019) 147-154.
54. [54] J.R. Perilla, B.C. Goh, C.K. Cassidy, B. Liu, R.C. Bernardi, T. Rudack, H. Yu, Z. Wu, K. Schulten, Molecular dynamics simulations of large macromolecular complexes, Curr Opin Struct Biol 31 (2015) 64-74.
55. [55] S.A. Hollingsworth, R.O. Dror, Molecular Dynamics Simulation for All, Neuron 99(6) (2018) 1129-1143.
56. [56] H. Monhemi, M.R. Housaindokht, A.A. Moosavi-Movahedi, M.R. Bozorgmehr, How a protein can remain stable in a solvent with high content of urea: insights from molecular dynamics simulation of Candida antarctica lipase B in urea : choline chloride deep eutectic solvent, Physical Chemistry Chemical Physics 16(28) (2014) 14882-14893.
57. [57] H. Monhemi, M.R. Housaindokht, A. Nakhaei Pour, Effects of Natural Osmolytes on the Protein Structure in Supercritical CO2: Molecular Level Evidence, The Journal of Physical Chemistry B 119(33) (2015) 10406-10416.
58. [58] H. Monhemi, M.R. Housaindokht, M.R. Bozorgmehr, M.S.S. Googheri, Enzyme is stabilized by a protection layer of ionic liquids in supercritical CO2: Insights from molecular dynamic simulation, The Journal of Supercritical Fluids 69 (2012) 1-7.
59. [59] M. Mohtashami, J. Fooladi, A. Haddad-Mashadrizeh, M.R. Housaindokht, H. Monhemi, Molecular mechanism of enzyme tolerance against organic solvents: Insights from molecular dynamics simulation, International Journal of Biological Macromolecules 122 (2019) 914-923.

60. [60] H. Monhemi, H.N. Hoang, D.M. Standley, T. Matsuda, M.R. Housaindokht, The protein-stabilizing effects of TMAO in aqueous and non-aqueous conditions, Physical Chemistry Chemical Physics 24(35) (2022) 21178-21187.
61. [61] Y. Zhao, X. Liu, J. Wang, S. Zhang, Insight into the Cosolvent Effect of Cellulose Dissolution in Imidazolium-Based Ionic Liquid Systems, The Journal of Physical Chemistry B 117(30) (2013) 9042-9049.
62. [62] H. Liu, K.L. Sale, B.A. Simmons, S. Singh, Molecular Dynamics Study of Polysaccharides in Binary Solvent Mixtures of an Ionic Liquid and Water, The Journal of Physical Chemistry B 115(34) (2011) 10251-10258.
63. [63] B. Derecskei, A. Derecskei-Kovacs, Molecular dynamic studies of the compatibility of some cellulose derivatives with selected ionic liquids, Molecular Simulation 32(2) (2006) 109-115.
64. [64] T.G.A. Youngs, J.D. Holbrey, M. Deetlefs, M. Nieuwenhuyzen, M.F. Costa Gomes, C. Hardacre, A Molecular Dynamics Study of Glucose Solvation in the Ionic Liquid 1,3-Dimethylimidazolium Chloride, ChemPhysChem 7(11) (2006) 2279-2281.
65. [65] T.G.A. Youngs, J.D. Holbrey, C.L. Mullan, S.E. Norman, M.C. Lagunas, C. D'Agostino, M.D. Mantle, L.F. Gladden, D.T. Bowron, C. Hardacre, Neutron diffraction, NMR and molecular dynamics study of glucose dissolved in the ionic liquid 1-ethyl-3-methylimidazolium acetate, Chemical Science 2(8) (2011) 1594-1605.
66. [66] J.-M. Andanson, E. Bordes, J. Devémy, F. Leroux, A.A.H. Pádua, M.F.C. Gomes, Understanding the role of co-solvents in the dissolution of cellulose in ionic liquids, Green Chemistry 16(5) (2014) 2528-2538.
67. [67] Z. Jarin, J. Pfaendtner, Ionic Liquids Can Selectively Change the Conformational Free-Energy Landscape of Sugar Rings, Journal of Chemical Theory and Computation 10(2) (2014) 507-510.
68. [68] V.S. Bharadwaj, T.C. Schutt, T.C. Ashurst, C.M. Maupin, Elucidating the conformational energetics of glucose and cellobiose in ionic liquids, Physical Chemistry Chemical Physics 17(16) (2015) 10668-10678.
69. [69] H. Liu, K.L. Sale, B.M. Holmes, B.A. Simmons, S. Singh, Understanding the Interactions of Cellulose with Ionic Liquids: A Molecular Dynamics Study, The Journal of Physical Chemistry B 114(12) (2010) 4293-4301.
70. [70] Y. Zhao, X. Liu, J. Wang, S. Zhang, Effects of Cationic Structure on Cellulose Dissolution in Ionic Liquids: A Molecular Dynamics Study, ChemPhysChem 13(13) (2012) 3126-3133.
71. [71] Y. Zhao, X. Liu, J. Wang, S. Zhang, Effects of anionic structure on the dissolution of cellulose in ionic liquids revealed by molecular simulation, Carbohydrate Polymers 94(2) (2013) 723-730.
72. [72] B. Mostofian, X. Cheng, J.C. Smith, Replica-Exchange Molecular Dynamics Simulations of Cellulose Solvated in Water and in the Ionic Liquid 1-Butyl-3-Methylimidazolium Chloride, The Journal of Physical Chemistry B 118(38) (2014) 11037-11049.
73. [73] F. Huo, Z. Liu, W. Wang, Cosolvent or Antisolvent? A Molecular View of the Interface between Ionic Liquids and Cellulose upon Addition of Another Molecular Solvent, The Journal of Physical Chemistry B 117(39) (2013) 11780-11792.
74. [74] H.M. Cho, A.S. Gross, J.-W. Chu, Dissecting Force Interactions in Cellulose Deconstruction Reveals the Required Solvent Versatility for Overcoming Biomass Recalcitrance, Journal of the American Chemical Society 133(35) (2011) 14033-14041.
75. [75] A.S. Gross, A.T. Bell, J.-W. Chu, Entropy of cellulose dissolution in water and in the ionic liquid 1-butyl-3-methylimidazolim chloride, Physical Chemistry Chemical Physics 14(23) (2012) 8425-8430.
76. [76] A.S. Gross, A.T. Bell, J.-W. Chu, Thermodynamics of Cellulose Solvation in Water and the Ionic Liquid 1-Butyl-3-Methylimidazolim Chloride, The Journal of Physical Chemistry B 115(46) (2011) 13433-13440.
77. [77] B.D. Rabideau, A. Agarwal, A.E. Ismail, Observed Mechanism for the Breakup of Small Bundles of Cellulose Iα and Iβ in Ionic Liquids from Molecular Dynamics Simulations, The Journal of Physical Chemistry B 117(13) (2013) 3469-3479.
78. [78] B.D. Rabideau, A.E. Ismail, Mechanisms of hydrogen bond formation between ionic liquids and cellulose and the influence of water content, Physical Chemistry Chemical Physics 17(8) (2015) 5767-5775.
79. [79] Y. Li, X. Liu, S. Zhang, Y. Yao, X. Yao, J. Xu, X. Lu, Dissolving process of a cellulose bunch in ionic liquids: a molecular dynamics study, Physical Chemistry Chemical Physics 17(27) (2015) 17894-17905.
80. [80] B. Doherty, O. Acevedo, OPLS Force Field for Choline Chloride-Based Deep Eutectic Solvents, The Journal of Physical Chemistry B 122(43) (2018) 9982-9993.
81. [81] T. Darden, D. York, L. Pedersen, Particle mesh Ewald: an Nlog(N) method for Ewald sums in large systems, J. Chem. Phys 98 (1993) 10089–10092.
82. [82] B. Hess, H. Bekker, H.J.C. Beredensen, J.E.M. Faraaije, LINCS: a linear constraint solver for molecular simulations, J. Comput. Chem. 18 (1997) 1463–1472.
83. [83] H.J.C. Berendsen, J.P.M. Postma, W.F. van Gunsteren, A. DiNola, J.R. Haak, Molecular dynamics with coupling to an external bath, J. Chem. Phys 81 (1984) 3684–3690.
84. [84] G. Bussi, D. Donadio, M. Parrinello, Canonical sampling through velocity rescaling, J Chem Phys 126(1) (2007) 014101.

85. [85] Y. Xie, H. Dong, S. Zhang, X. Lu, X. Ji, Effect of Water on the Density, Viscosity, and CO2 Solubility in Choline Chloride/Urea, Journal of Chemical & Engineering Data 59(11) (2014) 3344-3352.
86. [86] C. Florindo, F.S. Oliveira, L.P.N. Rebelo, A.M. Fernandes, I.M. Marrucho, Insights into the Synthesis and Properties of Deep Eutectic Solvents Based on Cholinium Chloride and Carboxylic Acids, ACS Sustainable Chemistry & Engineering 2(10) (2014) 2416-2425.
87. [87] G. Liu, H. Sun, G. Liu, H. Zhang, S. Yuan, Q. Zhu, A molecular dynamics study of cellulose inclusion complexes in NaOH/urea aqueous solution, Carbohydr Polym 185 (2018) 12-18.
88. [88] M. Brehm, M. Thomas, S. Gehrke, B. Kirchner, TRAVIS—A free analyzer for trajectories from molecular simulation, The Journal of Chemical Physics 152(16) (2020) 164105.
89. [89] E. Arunan, G.R. Desiraju, R.A. Klein, J. Sadlej, S. Scheiner, I. Alkorta, D.C. Clary, R.H. Crabtree, J.J. Dannenberg, P. Hobza, H.G. Kjaergaard, A.C. Legon, B. Mennucci, D.J. Nesbitt, Definition of the hydrogen bond (IUPAC Recommendations 2011), 83(8) (2011) 1637-1641.
90. [90] P. Muller, Glossary of terms used in physical organic chemistry (IUPAC Recommendations 1994), 66(5) (1994) 1077-1184.
91. [91] I. Pethes, I. Bakó, L. Pusztai, Chloride ions as integral parts of hydrogen bonded networks in aqueous salt solutions: the appearance of solvent separated anion pairs, Physical Chemistry Chemical Physics 22(19) (2020) 11038-11044.
92. [92] C. Xu, Q.G. Tran, D. Liu, C. Zhai, L. Wojtas, W. Liu, Charge-assisted hydrogen bonding in a bicyclic amide cage: an effective approach to anion recognition and catalysis in water, Chemical Science 15(39) (2024) 16040-16049.
93. [93] Y. Li, J. Wang, X. Liu, S. Zhang, Towards a molecular understanding of cellulose dissolution in ionic liquids: anion/cation effect, synergistic mechanism and physicochemical aspects, Chemical Science 9(17) (2018) 4027-4043.
94. [94] J. Zhang, J. Wu, J. Yu, X. Zhang, J. He, J. Zhang, Application of ionic liquids for dissolving cellulose and fabricating cellulose-based materials: state of the art and future trends, Materials Chemistry Frontiers 1(7) (2017) 1273-1290.
95. [95] M. Wohlert, T. Benselfelt, L. Wågberg, I. Furó, L.A. Berglund, J. Wohlert, Cellulose and the role of hydrogen bonds: not in charge of everything, Cellulose 29(1) (2022) 1-23.
96. [96] X. Yuan, G. Cheng, From cellulose fibrils to single chains: understanding cellulose dissolution in ionic liquids, Physical Chemistry Chemical Physics 17(47) (2015) 31592-31607.